

The Raft River Valley in south central Idaho is a downdropped, sediment filled basin. It is bounded on the east by the Black Pine Mtns. and the Sublette Range, on the west by the Jim Sage and Cotterell Mtns., and on the south by the Raft River Range. The valley opens onto the Snake River Plain to the north (Figure 1). The Raft River enters the basin at the south end of the Jim Sage Mtns. and flows northward. The present topography near the KGRA (Known Geothermal Resource Area) is characterized by coalescing alluvial fans fringing the relatively flat flood-plain of the Raft River.

The mountain ranges surrounding the KGRA vary compositionally and structurally. They are described initially to provide a regional geologic perspective. The Sublette Range and Cotterell Mountains are omitted since they have little direct influence on the KGRA.

#### BLACK PINE MTNS.

The Black Pine Mtns. bound the east side of the valley. They are 27 Km long and rise 1195 m. above the valley floor.

#### Stratigraphy

The range is composed of a sequence of late Paleozoic marine sediments, minor Tertiary volcanic sediments and minor Quaternary alluvial and colluvial sediments. The exact formation thicknesses and sequences are difficult to determine because of the tectonic nature of many unit boundaries (French 1975).

#### Devonian

Jefferson (?) Formation - This unit is approximately 122 m. of dolomitic limestone with interbedded quartzite and chert. It weathers light to dark-gray and outcrops near the center of Black Pine canyon. A bedding plane thrust fault is the top contact; the basal contact is not exposed (French 1975).

#### Mississippian

Milligan Formation - This unit is approximately 564 m. thick with an estimated maximum thickness of 640 m. The lithology is black carbonaceous argillite interbedded with quartzite and minor siltstone. This unit has absorbed more tectonic deformation than those above and below. Both contacts are tectonic. Exposures are in the southeast portion of the range.

White Knob Formation - This unit is comprised of two members. The lower is 500 m. of interbedded limestone, argillite, calcereous siltstone, sandy limestone and quartzite. The upper member is 240 m. of massive, bluegray limestone with interbeds of sandy limestone and siltstone. Both contacts are tectonic. Exposures are widespread in the south end of the range. (French 1975).

The USGS has mapped the Mississippian strata in the Black Pine Mtns., designating two units: an unnamed limestone and sandstone, and the Manning Canyon Shale (Armstrong, 1978). These correlate with the units mapped by French.

#### Pennsylvanian

Undifferentiated Unit - This unit as described by French, is 550 m. of sandy limestone, fine grained, calcereous sandstone, and quartzite. The upper contact is eroded away, the bottom contact is a bedding plane thrust fault. The USGS mapped large exposures of Pennsylvanian strata in the central and southern portion of the range. They assign this strata to the Oquirrh Fm. (Armstrong, 1968).

#### Tertiary

Tuffaceous sediments - The Tertiary is represented by thin layers of air fall tuff, weakly cemented tuffaceous silts, sands and conglomerate, and black to gray vitroplanes. Exposures are primarily around the north end of the range. (Armstrong, 1978). French correlates these sediments to the Tertiary Salt Lake Fm.

#### Quaternary

These deposits include exposures of the Lake Bonneville group on the southeast side of the range as well as colluvium, stream alluvium, landslide deposits and alluvial fans, mostly Pleistocene and Holocene in age.

#### Metamorphism

Low grade metamorphism is present in a few local outcrops in the south portion of the range. The Milligan Fm. is locally altered to slate and phyllite from contact and tectonic metamorphism. The White Knob Fm. is locally altered to marble by tectonic metamorphism.

### Mineralization

Mineralization accured in the southeast part of the range in two phases. The first produced mesothermal deposits in fractures related to Laramide structure. The second produced mesothermal and epithermal deposits in fractures related to Basin-and-range structure.

Two small igneous dikes were emplaced concurrently with the second phase of mineralization. These rocks, originally a diabase, are heavily altered.

### Structure

The structure in this range exhibits high angle Basin-and-Range normal faulting superimposed on older folds and thrust faults. Thrust faulting, dated Post Paleozoic, has moved younger strata over older. (French 1975).

## JIM SAGE MTNS

The Jim Sage Mtns. bound the west side of the valley. They are 29 Km long, and rise 667 m. above the valley floor. Two small blocks are separated from the south end of the range by an inferred right-lateral strike-slip fault (Williams et.al., 1974). The Raft River flows through this divide.

### STRATIGRAPHY

#### Tertiary

Salt Lake Fm. - The range is composed entirely of this formation. The upper member is gray to light green tuffaceous siltstone and sandstone with minor conglomerate composed of clasts of quartzite, dolomite, limestone, schist and rhyolite.

The middle volcanic member is composed of rhyolite flows, tuffaceous siltstone, and vitrophere breccia.

The lower member is gray to white, thin-bedded to massive, tuff and tuffaceous sandstone; white to light green shale and siltstone; and sparse beds of fine-grained conglomerate (Williams et.al, 1976).

#### Structures

The Jim Sage Mtns. are structurally simple; the range is a tilted antiform block, the crest very near the eastern margin creating steep scarps facing east and a gentle slope facing west (Anderson, 1931). Steep normal faults

located primarily along the range fronts are attributed to Basin-and-Range tensional forces.

### RAFT RIVER RANGE

The Raft River range forms the southern boundary of the valley. It is 40 Km long and rises 1250 m. above the valley floor. This range is the only east-west trending range in the area.

#### Stratigraphy

Stratigraphic units have been highly deformed and metamorphosed, drastically thinning or erasing them locally. Although many units are cut by thrust faults, younger formations were emplaced over older, so that the stratigraphic sequence is generally in order. (Compton, 1978).

#### Precambrian

Older Schist- This unit is composed of brown and silvery mica-rich schists. Relict features indicate the rocks were originally shale, argillaceous and feldspathic sandstone and siltstone, and pebbly to cobbly mudstone. These rocks are intruded by granitics and are apparently the oldest rocks in the range. Exposures occur widely throughout the range.

Metamorphosed Adamellite - These intrusive rocks are primarily made of adamellite grading upward into gneiss and schist, and locally accompanied by granodiorite. The rocks are exposed in most of the deep canyons in the range and are probably part of a 2,500 my. - old basement present in northwestern Utah and adjacent Idaho (Armstrong and Hills, 1967).

Elba Quartzite - This unit consists primarily of white, tan and green quartzite with lenses of white quartz-pebble-conglomerate. The unit is widely variant over the range both in lithology and thickness. Exposures are widely scattered.

Schist of the Upper Narrows - This unit is characterized by dark-brown or gray rocks that form slabby outcrops. Most abundant are fine to medium grained biotitic schist and fine grained gneiss. The unit is fully exposed in the Upper Narrows of Raft River in the northwest part of the Yost Quadrangle and all but the upper part of the schist is exposed in the Park Valley Quadrangle.

Quartzite of Yost - This quartzite is approximately 120 m. thick and is well exposed south of Village of Yost. It is characteristically white, however green quartzite, colored by chromian mica, and greenish-gray variants can be found. This unit is not exposed in the Park Valley Quadrangle.

Schist of Stevens Springs - This unit is 150 m. thick south of the town of Yost and 90 m. thick elsewhere. The main rock type is fine grained muscovite-quartz schist that is interlayered with homogenous muscovite and graphitic phyllites and schists.

### Cambrian

Quartzite of Clarks Basin - This quartzite is about 120 m. thick where it is complete. It is composed of gray to white flaggy quartzites, and forms parts of thrust sheets on the north-west and south-east flanks of the range.

Schist of Mahogany Peaks - This schist ranges from 15-90 m. thick and is exposed only on the southeast and northwest flanks of the range. The rocks are dark in color, lack bedding, and contain abundant mica, garnet and staurolite.

### Ordovician

Metamorphosed Pogonip Group - The marbles, schist and quartzites of this group are the most abundant rocks in the relics of a thrust sheet that must have once extended over the entire range. Two lithologic facies are represented, a metamorphosed limestone which makes up the lowest thrust sheet of Bald Knoll, and gray laminated marbles that are widespread along the north side of the range.

Metamorphosed Eureka Quartzite - This white quartzite is 120 m. thick and is exposed widely, lying conformably over the Pogonip group limestones.

Metamorphosed Fish Haven (?) Dolomite - This unit is characterized by silver-gray laminated dolomite that is overlain and commonly mixed with brecciate pale-tan dolomite. The unit is 90 m. thick in the northwest part of the Park Valley Quadrangle.

### Mississippian

Metamorphosed Chainman or Diamond Peak Formation - This unit is composed of dark-gray phyllite, sooty black limestone, and gray sandstone that forms

lenses and sheets up to 90 m. thick. Some are in normal contact with the Oquirrh but most are in slices bounded by thrust faults.

### Pennsylvanian

Oquirrh Formations - This unit formed a thrust sheet that once covered the entire Park Valley Quadrangle. The unit is highly deformed, but the thickest remnant is 300 m. The rocks are mainly sandstone and limestone that are locally metamorphosed.

### Tertiary

Mudstone, sandstone and conglomerate - These rocks are several thousand feet thick and lie along the entire north and south edges of the range. Exposures are limited because of the easily erodable nature of the rocks. The sequence is conglomeratic near the bottom, made of detritus from the Oquirrh Fm., grading upward to sandy and silty rocks containing abundant silicic ash.

Igneous rocks - There are several occurrences of igneous rocks in the range; an irregular lamphoplyre dike, probably Miocene, cuts the Elba Quartzite on the northwest flank of the range, three small diabase patches underlie the lowest thrust sheet near the top of the range, and flows of gray glassy dacite lie mainly on Oquirrh Fm. rocks east of Stardrod.

### Quaternary

Quaternary rocks consist of stream deposits, landslides, colluvium and alluvium.

### Metamorphism

The metamorphism in the range is the type normally associated with the Precambrian of the area, however, here it is apparently of tertiary age. (Compton, 1975). There were two stages of metamorphism, the first ended  $38.2 \pm 2.0$  my ago and second ended  $24.9 \pm 0.6$  my ago (Compton, 1977). Metamorphic grade increases downward and westward in the autochton (Precambrian Adamellite) and downward in the allochthons.

### Structure

The Raft River range exposes two allochthorous sheets composed of Precambrian, Paleozoic and Triassic sediments that were transported tens of kilometers on low-angle faults. Transport was westward and northward during

the two stages of metamorphism, and eastward after metamorphism, (Compton, 1977). Three sets of folds formed during metamorphism range from upright to recumbant. Most are strongly overturned to the northwest. A fourth set of folds, formed after metamorphism, vary in form and trend suggesting complex and localized movement. The orientation of these folds, and some high grade metamorphism in the allochthons which overlie low grade metamorphism in the autochthons indicate the later eastward movement (Compton, 1977).

Compton suggests that deformation was caused by gravity gliding on a broadly heated dome. The crest of the dome probably shifted causing the different directions of movement. Parts of the dome sagged forming broad basins 12 my ago. The coarse sediments and tuffs that filled these basins were then overrun by the eastward motion of the allocthonous sheets. The present Raft River Range formed during Pliocene time as a broadly arched anticline oriented east-west.

## INJECTION STUDIES

Because of environmental concerns associated with surface disposal of geothermal waters, subsurface injection of the cooled fluid from the 5MW plant is planned at the Raft River KGRA.

Two studies were carried out to evaluate potential problems of aquifer clogging during injection. The first test involved the evaluation of water compatibility, that is, the effects of mixing geothermal waters from two or more wells on the quantity of chemical precipitates formed. This indicates the potential for clogging receiving zones in injection wells due to chemical reactions. In a second test, the quantity and size distribution of suspended particulate matter was measured. This gives the potential for clogging due to physically transported material, and indicates filter sizes needed to remove particulate matter.

### Water Compatibility

The water compatibility test is an empirical determination of the synergistic effects of mixing water from two or more wells. The results indicate the changes in suspended solids in the mixtures due to chemical reactions between the waters. Increases in suspended solids from precipitation reactions is an important criteria limiting the feasibility of injection. Injection of excessive particulate matter, or the formation of chemical precipitates in an aquifer can cause serious plugging problems in injection wells.

### Experimental Procedure

Experiments were carried out at two temperatures to simulate two possible injection schemes. One set of experiments was carried out at  $\approx 20^{\circ}$ , the temperature expected for injection of water from holding ponds, and the second set was done at  $\approx 70^{\circ}\text{C}$ , to simulate injection of water directly from the 5MW facility. Water samples were collected from wells RRGE-1, RRGE-2, RRGE-3, RRGP-5, and RRG1-6, and filtered through 0.45 micron membrane filters to remove any suspended solids. Mixtures of one liter total volume were prepared by mixing all possible permutations of water combinations using equal portions of each water in the mixture. For example, a mixture of two craters could contain 500 mls of each. Control samples of unmixed water from each well were also included. Samples could not be collected from wells RRGP-4

~~TABLE~~

Table — WATER COMPATIBILITY FOR GEOTHERMAL } lower case letters  
 WELLS 1, 2, 3, 5, AND 6  
 RRG-

Sample Mixtures RRG-	Samples Collected Through a Condensor			
	Temp. 20 °C		Temp. 70 °C	
	Calculated (mg/l)	Actual (mg/l)	Calculated (mg/l)	Actual (mg/l)
1		0.6		0.0
2		1.2		0.0
3		2.4		0.5
5		0.1		0.0
6		4.1		2.4
1-2	0.9	0.1	0.0	0.0
1-3	1.5	1.1	0.3	0.0
1-5	0.4	1.1	0.0	0.0
1-6	2.4	0.9	1.2	0.0
2-3	1.8	0.5	0.3	0.0
2-5	0.7	0.2	0.0	0.0
2-6	2.7	2.6	1.2	1.2
3-5	1.3	0.1	0.3	0.0
3-6	3.3	3.6	1.5	-
5-6	2.1	2.3	1.2	0.6
1-2-3	1.4	1.9	0.2	0.0
1-2-5	0.6	0.7	0.0	0.0
1-2-6	2.0	1.2	0.8	0.0
1-3-5	1.0	0.7	0.2	0.0
1-3-6	2.4	1.6	1.0	0.0
1-5-6	1.6	1.6	0.8	0.0
2-3-5	1.2	-	0.2	0.0
2-3-6	2.6	0.0	1.0	0.0
2-5-6	1.8	1.1	0.8	1.2
3-5-6	2.3	1.5	1.0	1.0
2-3-5-6	2.0	2.5	0.7	0.2
1-3-5-6	1.8	0.9	0.7	0.0
1-2-5-6	1.5	2.6	0.6	0.0
1-2-3-6	2.1	1.7	0.7	0.5
1-2-3-5	1.1	0.0	0.1	0.0
1-2-3-5-6	1.7	0.7	0.6	0.0
mean <sup>1</sup>		1.25		0.19
Standard <sup>1</sup> Deviation		0.94		0.39
n <sup>1</sup>		25		25

<sup>1</sup> of mixtures only

- missing sample

and RRG1-7, so they were not included in the analysis.

After 24 hours at 20°C or 70°C, the mixtures were filtered through tared 0.45 micron filters and the filters dried at 95°C for one hour. Residue and filter were then weighed on an analytical balance and the residue calculated by difference.

## Results

The quantity of precipitate expected in the mixed samples, assuming no synergistic effects, was calculated by summing the products of the solids formed in the control samples times the fraction of the sample in the mixture. If there are no synergistic effects of mixing, the measured and calculated amounts of precipitate should be equal.

Results of the measurements and calculations are shown in Table \_\_. The columns headed "actual" represent the weights of precipitated solids determined from filtering and weighing. The columns headed "calculated" represent the predicted quantity of precipitate assuming no interactive effects in the mixtures.

To determine if there is a significant effect on the quantity of precipitated solids due to mixing, differences between calculated and actual weights of solids were calculated. If there are no synergistic effects, the mean of the differences should equal zero. A significant positive or negative difference would indicate an enhancement or inhibition of solids formation, respectively. For the 25 mixtures held at 20°C, the average difference is -0.44 mg/l with a 95% confidence interval from -0.78 to -0.10 mg/l. For the 25 mixtures held at 70°C, the average difference is -0.37 mg/l with a 95% confidence interval from -0.53 to -0.21 mg/l. There is a significant inhibition effect due to mixing, with mixed waters producing an average of about 0.4 mg/l less precipitated solids than expected from the amount of solids precipitated from the unmixed waters.

To assess the effects of temperature on the quantity of precipitate formed, the average amount of filtered solids for the mixed samples at the two temperatures was compared. For the mixtures held at 20°C, the average was 1.25 mg/l with a standard error of the mean of 0.19 mg/l. For the samples held at 70°C, the average amount of precipitate formed was 0.19 mg/l with a standard error of 0.08 mg/l. The amount of solids formed in mixtures held

at 20°C was significantly greater than for samples held at 70°C.

Examination of the amounts of solids precipitated from the unmixed samples shows that wells RRGE-1, RRGE-2 and RRGP-5 produce relatively little precipitate. Wells RRGE-3 and RRG-6 produce from two to three times as many solids as the other wells. Hot waters injected into RRG-6 directly from the 5MW plant can be expected to form about 0.2 mg/l of solids on the average.

### Conclusions

Mixing of water from wells RRGE-1, RRGE-2, RRGE-3, RRGP-5, and RRGE-6 show no incompatibility. In fact, water mixtures show less formation of precipitated solids than anticipated from quantities formed from unmixed waters. There is a significant inhibition effect, with about 0.4 mg/l fewer solids formed than estimated. Samples held at 70°C showed significantly less precipitate formation than those held at 20°C. Injecting water directly upon leaving the power plant would minimize the formation of suspended solids. Even with only 0.2 mg/l of chemical precipitate formed, 2.2 Kg/day of solids would be injected into the aquifer assuming an average flow of 126 l/sec.

### Filter Studies

Studies were carried out to evaluate the amount and particle size distribution of suspended solids in geothermal water from the Raft River KGRA. Injection of excessive suspended solids can cause clogging of injection wells, ruining their utility. Analysis of the size distribution of suspended solids would permit the sizing of filter screens for the injection system. Particle size distributions were determined for water from wells RRGE-2 and RRGE-3. Total solids were monitored during two additional tests.

### Experimental Procedure

The filtering apparatus used in the tests consisted of a series of stainless steel filters in the following sizes and order - 230, 140, 90, 60, 15, and 2 microns. A 0.45 micron membrane filter was also used. The 230 and 140 micron filters were used in only one test. For determining total suspended solids, the 2.0 micron filter was used alone. The filters were

Particle Size Range (microns)	RRGE-2 - 5/18/78 (mg/l)	@ RRGE-3 RRGE-3 3/21/78 (mg/l)	@ RRGE-3 RRGT-4 3/22/78 (mg/l)
0.45 - 2	0.08	0.87	1.49
2 - 15	0.09	2.12	8.12
15 - 60	0.10	0.56	6.54
60 - 90	0.11	0.51	6.41
>90	-	0.72	51.6
90-140	0.04	-	-
140-230	0.00	-	-
>230	0.06	-	-
TOTAL	0.48	4.78	74.16

Table \_\_\_\_\_ Particle size distributions of suspended solids in geothermal waters from Raft River KGRA.

placed in stainless steel filter holders, and from 20 to 100 liters of water passed through the series. Filters were dried at 105°C for three hours and weighed on an analytical balance. The quantity of suspended solids was determined by subtracting the tared weight of the filter.

## Results

Table \_\_ shows the weights of suspended solids collected on filters of various pore sizes from wells RRGE-2 and RRGE-3. The third column represents water from well RRGE-3 collected just before injection into well RRG-4, after it had passed through the pipeline system connecting the two wells. The quantity of suspended solids from well RRGE-3 is much higher than from well RRGE-2. A major source of suspended material is from the distribution system itself. The distribution of particle sizes shows that almost all of the particles from the wells are less than 90 microns in diameter. Particles picked up in the distribution system are larger, and are larger than 90 microns.

To test for temporal effects, well RRGE-2 was tested for total suspended solids every 24 hours for five days during an injection test of well RRG-6. There was a general increasing trend in solids from 0.17 mg/l the first day to just over 1 mg/l on the fifth day. Concentrations were in the same range as for the earlier test on well RRGE-2. Five days, however, was not sufficient time for the solids to stabilize, and the long term suspended solids concentration can not be predicted from this data.

Suspended solids were determined during a fourth injection test, when water from the holding pond at well RRGE-1 was injected into well RRG-7. The average concentration of suspended solids in this water was 34.8 mg/l, much higher than produced from either well RRGE-2 or RRGE-3.

## Conclusions

Knowing particle size of the undissolved solids in water to be injected is important in determining filter size, designing filtering systems, and determining the impact on the production zones in an injection well. The studies of particle size conducted on the injection of well RRGE-2 water into well RRG-4 and the injection of well RRGE-3 water into well RRG-4 indicated that  $\approx$  80% of the undissolved solids were smaller than 90 microns.

Also in well RRGE-3, 35.5% of the undissolved solids were between 2.0 and 15.0 microns. This would require very small filters to remove the major portion of the undissolved solids. Large amounts of suspended solids are picked up in the pipeline carrying water to the injection well. About 94% of the solids measured at the injection of RRGI-4 were from this source. Without removal of these suspended solids, 800 kg of solids per day could be injected into the ground. Even with installation of 90 micron filters, however, 245 kg of solids per day would be injected assuming a plant operating flow of 126 l/sec.. This is a rather large quantity of solids, and could significantly interfere with injection of the spent fluids.

The filter study of the water from well RRGE-2 being injected into well RRGI-6 indicated a trend of increasing amounts of undissolved solids as the test progressed. Unfortunately, the test was terminated before it could be determined if the increase in solids was the result of the wellbore being flushed of residual materials.

Water injected from holding ponds was very much higher in suspended solids than water pumped directly from wells. Holding wastes in ponds could significantly increase the quantity of solids needed to be filtered out before injection, unless an effort is made to flocculate and remove these solids in the pond.

## INTRODUCTION

A number of studies involving water chemistry were conducted to support the development of the Raft River geothermal field. Geothermal waters frequently have high levels of dissolved solids (Ellis and Mahon, 1977), which require characterization to anticipate potential problems associated with utilization of the resource. These problems range from corrosion and scaling to environmental concerns about disposal of geothermal fluids.

Because of the relatively high dissolved solids content of water from the Raft River KGRA, subsurface reinjection of the spent geothermal waters is required by the Idaho Department of Water Resources. Most of the geochemical studies involve potential problems arising from this reinjection requirement. Corrosion and scaling problems in the plant are being investigated by the Conversion Technology Group.

The most important reinjection concern is the effect that injection of cooled waters will have on the geothermal resource. The effects of reinjection of geothermal waters on the quality of ground waters in the valley is also of concern. Salt buildup in soils is a critical problem where agriculture is supported by irrigation in semi-arid areas (El - Ashry, 1980). Large increases in dissolved solids of shallow ground waters in the Raft River Valley from reinjection could interfere with the farming economy of the area. Additional reinjection problems can occur from plugging of injection wells. In geothermal systems this can come from suspended solids or from chemical precipitates.

To define the hydrologic system of the Raft River KGRA, a conceptual model of the field was developed. This model shows sources of water and heat to the aquifer and directions of flow. This model can be used to evaluate the locations of the injection wells at Raft River. Additional studies described here include studies about the reinjectability of the fluids. This includes quantity and size distribution of suspended solids, and the formation of chemical precipitates from waters during mixing.

Finally, a chemical logging technique is described that was developed during drilling at the Raft River KGRA. This logging technique can be used to locate geothermal aquifers while drilling is in progress. The technique is capable of anticipating hot aquifers before they are penetrated by the drill string. This would permit casing to be run before high pressure aquifers were intercepted that would require killing or cementing the well.

#### WELL CHEMISTRY

As each of the geothermal wells was completed, it was developed and tested for yield. Water samples were collected for chemical analysis at this time. Additional samples were collected from the wells during pump tests, or during production runs. Seven monitor wells were drilled to follow water level and chemical changes in shallow ground water in the vicinity of the KGRA. In addition to these wells drilled in conjunction with the Raft River site, analyses have been made on domestic and irrigation wells in the area. Chemical analyses from these groups of wells have been compiled into a computerized data base to permit easy access to the data.

Discussion of well chemistry in this section is limited to the seven deep geothermal wells. The chemistry of the monitor well network is covered by Spencer and Callan (1980), and of the general shallow ground water by Walker, and others (1970).

Table \_\_\_ shows a selected analysis from each of the wells used in the development of the geochemical model in the next section. The analyses in this table are averages of the most consistent chemical analyses from each of the wells, and were selected on the basis of yielding results close to electrical neutrality. For the seven geothermal wells, the seven monitor wells, and the three U.S. Geological Survey wells, the temperature is the bottom hole temperature obtained from geophysical logs. Other temperatures are as measured in the water during sampling. The silica and Na-K-Ca temperatures were calculated for wells that had warm water temperatures using the equations given by Fournier (1977).

All the deep geothermal wells are sodium chloride type waters, based on the predominant cation and anion in terms of milliequivalents per liter (meg/L). The sodium ranges from 83 to 91 percent of the cations, and chloride from 92 to 99 percent of the anions. The waters are all low in alkalinity, ranging from 26 to 60 mg/L as  $\text{CaCO}_3$  (32 to 73 mg/L as  $\text{HCO}_3^-$ ). There is a great deal of variation in the total amount of dissolved solids among the wells.

Wells RRGE-1, RRGE-2, and RRGP-5 are towards the northwest side of the KGRA, and were located to intercept the Bridge Fault at depths where hot water was anticipated. These wells are similar in dissolved solids content, temperature, and chemical character. Contents of dissolved chemical species are relatively low, with specific conductivities ranging from 2500 - 2800  $\mu\text{mhos}$ . These wells also have the highest fluoride contents, with greater than 7 mg/L in all three.

Wells RRG-6 and RRG-7, injection wells, are located to the southwest, and were completed at more shallow depths than the production wells so as not to interfere with the geothermal resource. These wells have very high dissolved solids contents, most of which is sodium and chloride, and are relatively low in fluoride, having 5.7 and 4.9 mg/L for RRG-6 and RRG-7 respectively. The temperature of these wells is also much lower than the others, being almost half that of the maximum measured in RRGE-3.

Wells RRGE-3 and RRGP-4 are intermediate in location and dissolved solids between the wells along the Bridge Fault, and those in the central-valley area. Well RRGE-3 has the hottest downhole temperature at 149<sup>o</sup>.

Calculated temperatures from geochemical thermometers give temperatures that fall within a fairly narrow range, and are close to temperatures measured in the geothermal wells. Calculated Silica temperatures indicate that the maximum temperatures in the reservoir may be from 10 to 20<sup>o</sup>C warmer than so far encountered in wells. Temperatures calculated from the Na-K-Ca geothermometer generally give temperatures from 30 to 40<sup>o</sup>C warmer than measured in wells. The general agreement between measured and calculated temperatures indicates that the wells are probably tapping about the hottest water available.

Well ID	RRGE-1	RRGE-2	RRGE-3	RRGP-4	RRGP-5	RRGI-6	RRGI-7
Well Depth (m)	1521	1994	1789	1654	1497	1176	1185
Casing Depth (m) ①	1105	1289	1293	1054	1039	509	623
T(°C)	141	144	149	142	135	71	78
SpC (MWhhos)	2800	2500	8000	4050	2700	10800	12000
PH (Units)	7.3	7.1	6.9	7.2	7.5	7.2	-
Ca <sup>2+</sup>	56	42	224	86	41	171	350
Mg <sup>2+</sup>	0.6	0.1	0.5	-	0.1	1.4	1.5
Sr <sup>2+</sup>	1.4	1.2	5.2	6.4	1.2	8.0	-
Na <sup>+</sup>	455	441	1194	753	484	2200	2200
K <sup>+</sup>	34	38	105	-	31	32	-
Li <sup>+</sup>	1.6	1.1	3.1	3.1	1.6	5.1	-
HCO <sub>3</sub> <sup>-</sup>	41	41	44	42	35	73	32
SO <sub>4</sub> <sup>2-</sup>	36	53	60	-	40	60	64
Cl <sup>-</sup>	776	708	2260	1400	800	3640	4000
F <sup>-</sup>	7.9	8.7	4.9	6.3	7.2	5.7	4.9
SiO <sub>2</sub>	121	131	158	104	133	94	83
T(°C) calc. from SiO <sub>2</sub>	148	153	164	136	154	134	127
T(°C) calc. from Na & Ca	173	183	187	-	169	114	-

① Depth to bottom of casing or to first perforations

Well ID	MW-1	MW-2	MW-3	MW-4	MW-5	MW-6	MW-7
Well Depth (m)	399	174	153	305	152	305	152
Casing Depth (m)	369	154	140	225	124	274	140
T(°C)	74	106	71	98	29	44	35
SpC (Mmhos)	11400	4400	6200	7800	2200	7600	2300
pH (units)	7.6	7.4	7.5	7.7	7.6	7.3	7.6
Ca <sup>2+</sup>	215	125	155	160	107	207	95
Mg <sup>2+</sup>	0.4	0.5	6.3	0.6	25	2.4	20
Sr <sup>2+</sup>	6.3	3.6	1.9	1.4	0.9	1.4	0.9
Na <sup>+</sup>	2220	1000	1400	1520	280	1570	333
K <sup>+</sup>	30	25	65	31	14	56	14
Li <sup>+</sup>	3.7	2.5	3.0	3.7	0.3	3.1	0.6
HCO <sub>3</sub> <sup>-</sup>	25	26	47	27	120	50	125
SO <sub>4</sub> <sup>2-</sup>	66	57	60	53	27	73	33
Cl <sup>-</sup>	3680	1740	2460	2610	610	2770	650
F <sup>-</sup>	3.4	5.4	5.4	5.6	0.6	4.9	1.1
SiO <sub>2</sub>	80	87	60	67	34	85	40
T(°C) calc. from SiO <sub>2</sub>	125	130	111	116	—	—	—
T(°C) calc. from Na-K-Ca	110	128	160	123	—	—	—

Well ID	BLM <sup>②</sup>	CROOK <sup>③</sup>	USGS-1	USGS-2	USGS-3	155-26E 23ABD1	155-26E 23DDD1
Well Depth (m)	126	165	336	243	434	110	78
Casing Depth (m)	—	—	—	64	60	—	—
T(°C)	93	97	28	55	89	29	42
SpC (Mmhos)	3000	5800	7400	1960	5900	4500	3900
pH (units)	7.4	7.7	7.8	7.7	7.7	7.6	7.1
Ca <sup>2+</sup>	44	130	230	51	57	97	104
Mg <sup>2+</sup>	0.7	0.8	2.5	4.0	0.5	5.0	8.0
Sr <sup>2+</sup>	1.5	2.8	1.7	0.3	2.0	—	—
Na <sup>+</sup>	577	1020	1500	370	1270	766	644
K <sup>+</sup>	21	32	200	34	14	20	18
Li <sup>+</sup>	1.4	2.6	0.9	6.6	1.7	1.9	1.1
HCO <sub>3</sub> <sup>-</sup>	49	34	100	216	77	155	168
SO <sub>4</sub> <sup>2-</sup>	65	56	45	55	54	96	57
Cl <sup>-</sup>	890	1750	2800	520	2040	1270	1100
F <sup>-</sup>	7.6	6.2	3.2	2.5	4.8	5.1	4.5
SiO <sub>2</sub>	74	86	85	88	54	61	58
T(°C) calc. from SiO <sub>2</sub>	120	127	—	130	105	—	—
T(°C) calc. from Na-K-Ca	144	138	—	182	103	—	—

② This well was drilled in the 1920's, and is called the Bridge well by the USGS, a well was drilled nearby in 1974 and is called the BLM offset

③ This well was previously owned by Crank, and is referred to by that name in earlier publications

Well ID	155-26E 24BAD1	155-26E 24BCB1	155-26E 24CAD1	155-26E 24DCC1	155-26E 26CAB1	155-26E 27DCC1	155-27E 19CCC1
Well Depth (m)	80	69	—	—	—	66	124
Casing Depth (m)	—	—	—	—	—	—	—
T(°C)	27	24	28	32	24	16	19
SpC (Mmhos)	2500	2400	2200	3300	3800	1400	2870
PH (units)	7.2	7.4	7.3	7.5	7.9	7.7	7.1
Ca <sup>2+</sup>	106	60	121	160	57	59	130
Mg <sup>2+</sup>	15	8.0	17	25	5.0	12	20
Sr <sup>2+</sup>	—	—	—	—	—	—	—
Na <sup>+</sup>	370	420	294	430	695	230	402
K <sup>+</sup>	13	11	13	17	13	9	20
Li <sup>+</sup>	0.8	0.9	0.6	0.8	1.5	0.3	0.8
HCO <sub>3</sub> <sup>-</sup>	200	200	216	150	125	250	235
SO <sub>4</sub> <sup>2-</sup>	61	62	69	76	58	62	75
Cl <sup>-</sup>	640	610	535	910	1080	315	750
F <sup>-</sup>	2.0	5.5	1.6	2.5	5.5	2.5	2.3
SiO <sub>2</sub>	53	55	44	59	59	53	58
T(°C) calc. from SiO <sub>2</sub>	—	—	—	—	—	—	—
T(°C) calc. from Na+K+Ca	—	—	—	—	—	—	—

## GEOCHEMISTRY OF GROUND WATER

The chemical composition of a ground water is related to the hydrology of the ground-water system. Waters from different source areas, variations in lithology along flow paths, and in geothermal reservoirs, variations in temperature history, produce differences in chemical compositions. By using the chemistry as a tracer for waters, the sources and flow paths may be discernible. A conceptual model of the flow system can be developed from this information.

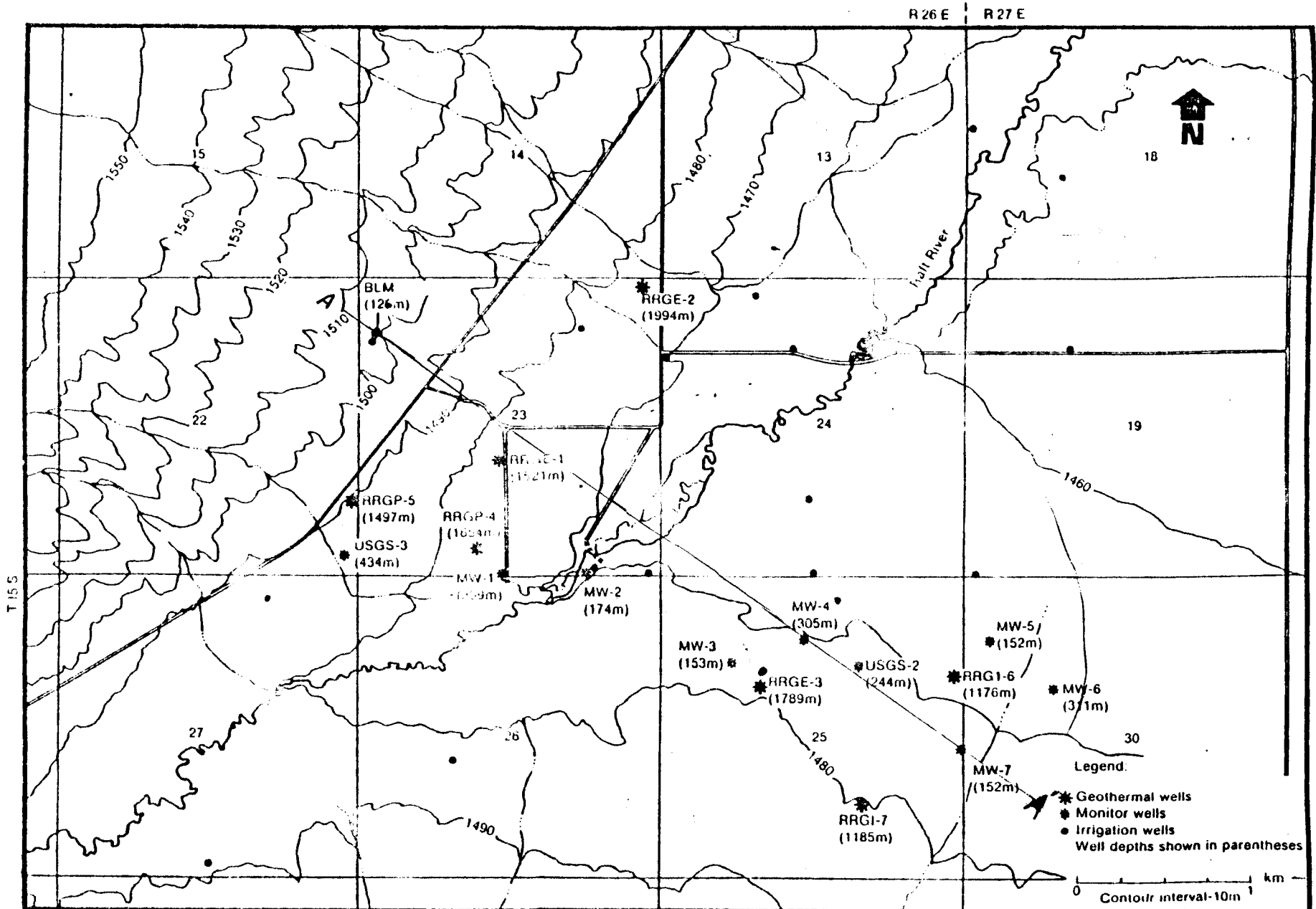
Because of the need to predict the effects of withdrawal and injection of geothermal fluids on the chemical quality of aquifers near the Raft River KGRA, the chemical data was used to develop a conceptual model of the area.

### Distribution of Chemical Species

The spatial distribution of chemical species is illustrated by contouring data collected from wells. Contouring requires subjective interpretation of data, and other interpretations than those presented are possible. There is adequate control in shallow ground water around the Raft River KGRA for the preparation of map views of the shallow ground water. Most of the data from the deeper zones falls in a narrow band along a northwest-southeast line between the BLM well and monitor well #7 (MW-7) (Figure \_\_). While this does not give adequate horizontal control for contouring, it is amenable to display in cross-section format. There is a lack of information about deep formation waters in the middle of the cross section (between RRGP-4 and RRGE-3), so the data from RRGE-3 have been weighted heavily in the contouring.

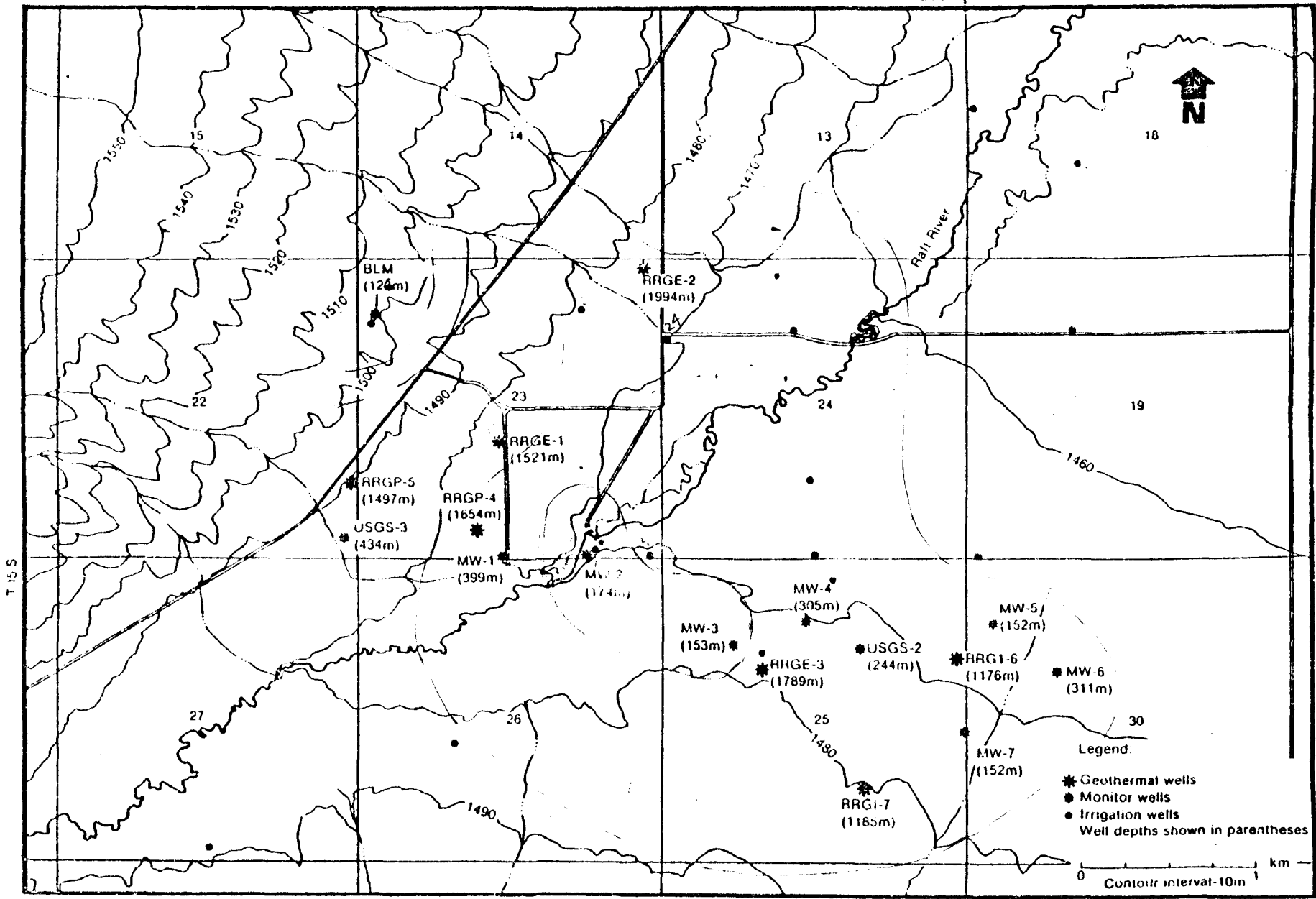
### Map View

Figure \_\_ shows the areal distribution in spl of shallow ground water (depth <200m) in the vicinity of the Raft River KGRA. Background conductance levels are less than 2000  $\mu$ mhos, with some wells having conductivities as low as 1000  $\mu$ mhos. Specific conductivities of ground water are higher over the geothermal resource, reaching a maximum of about 6000  $\mu$ mhos southwest of the river. This same area also exhibits the highest temperatures for shallow ground water (Figure \_\_).



SPECIFIC CONDUCTANCE OF SHALLOW (<200m) GROUND WATER IN THE VICINITY OF THE KAFT RIVER KGRA

R 26 E | R 27 E



TEMPERATURE OF SHALLOW (<200m) GROUND WATER IN THE VICINITY OF THE RAFT RIVER KGRA.

IN 11 A 10 93

The BLM well, to the northwest, is also quite warm, but appears isolated from the warm waters near the center of the area by cooler waters. This zone of high conductivity and temperature in the ground water indicates a plume of geothermal water rising above the hot zone and mixing with shallow ground waters.

### Cross Sections

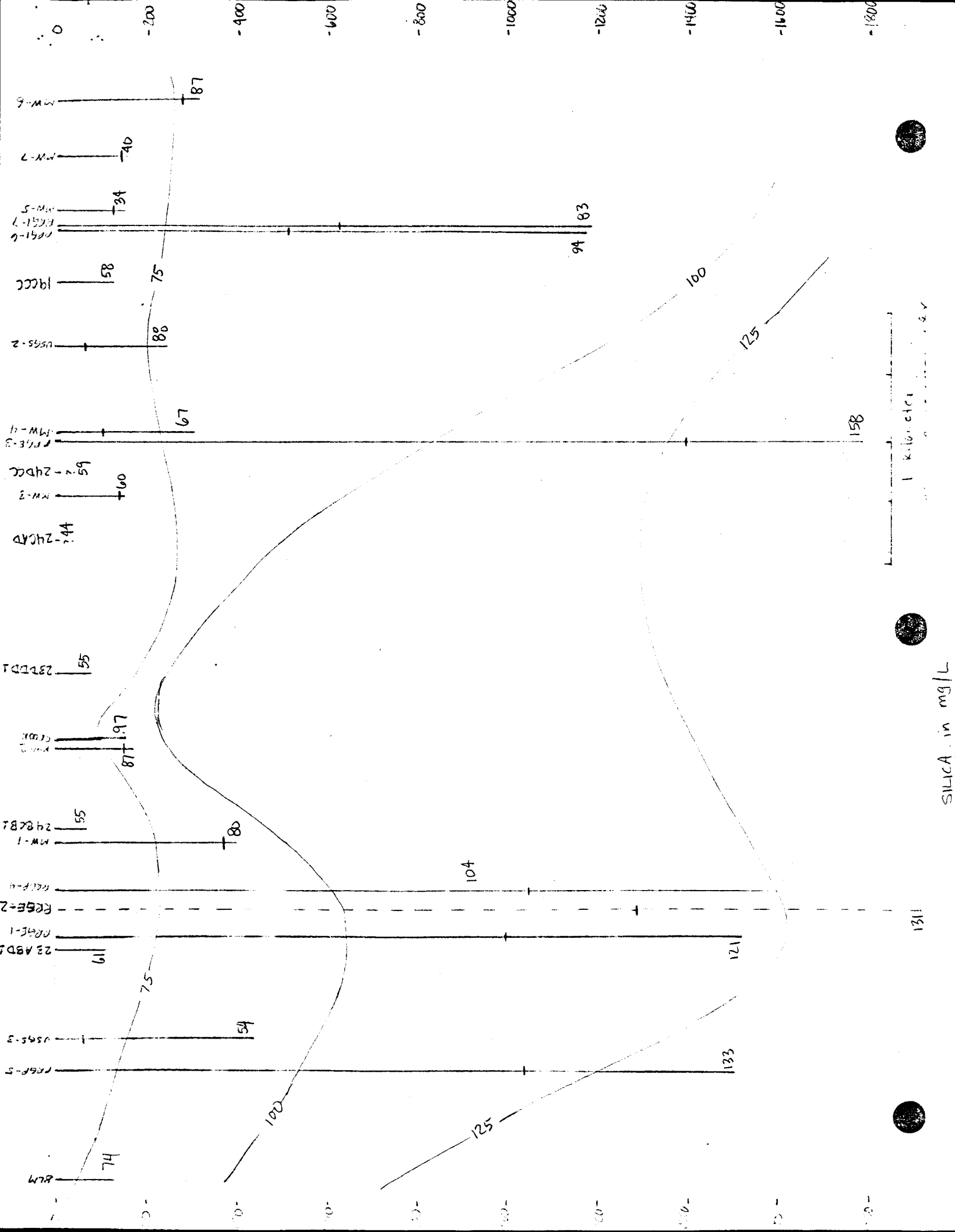
A cross section through the Raft River KGRA (location shown as A-A' in Figure \_\_) shows variations in chemistry and temperature with depth. Wells projected onto the cross section produce some variations due to lateral variations in chemistry. Well RRGE-2 is dashed in the cross section because of its distance from the cross section. It was included to add additional information at depth.

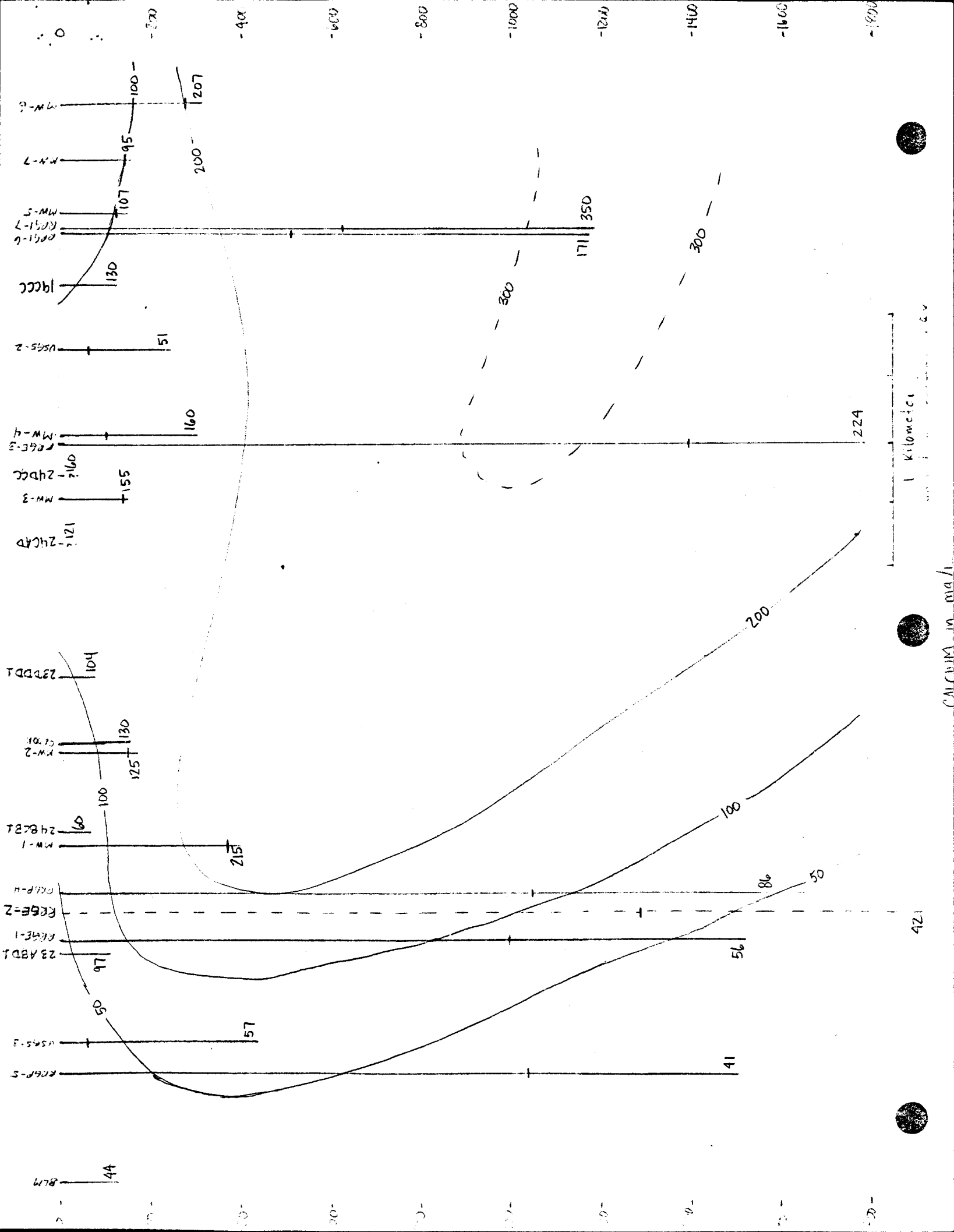
Chemical and temperature cross sections generally show one of two patterns. One type of pattern is exhibited by sp1 (Figure \_\_), with a plume of high conductivity waters moving in from the southeast through wells RRG1-6 and RRG1-7. This plume moves upwards to near the surface at MW-1. A second pattern is shown by temperature measurements. These temperatures are from downhole temperature logs for the geothermal wells and monitor wells, and from measured water temperatures for the other wells. Temperature contours show a different pattern, with contours dipping steeply to the southeast and approaching the surface near the Crook and BLM wells.

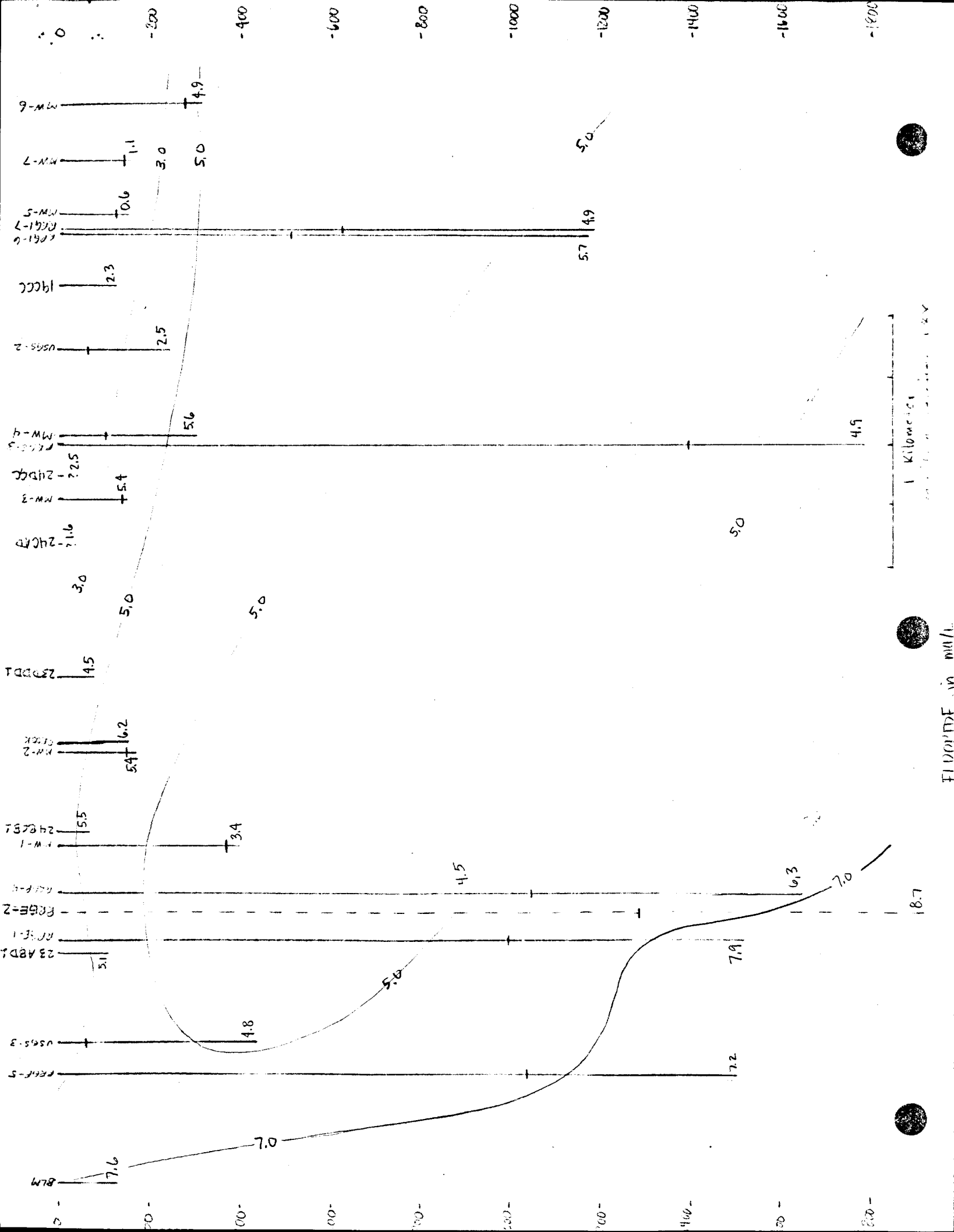
Other chemical species tend to show one of these two patterns. Silica, (Figure \_\_) which is controlled by the temperature effects on the solubility of quartz, closely follows the appearance of the temperature cross section. The dissolved species closely follow the appearance of the conductive cross section. Calcium, for example, also shows the plume of high concentrations moving in from the southeast. Fluoride shows a unique distribution in cross section. While a plume from the southeast is still present, concentrations of fluoride in this plume are lower than in immediately surrounding areas. The highest fluoride concentrations occur in deep geothermal waters to the northwest.











Fluorite commonly controls the maximum fluoride concentrations in hydrothermal waters (Ellis and Mahon, 1977), and may be controlling the low fluoride concentrations in the southeast of the geothermal field. Figure \_ shows a plot of calcium versus fluoride, with a dashed line representing the expected calcium and fluoride concentrations in equilibrium with fluorite at about 125°C (Kharaka and Barnes, 1973). Because of temperature variations and variations in ion activities due to ionic strength variations, this dashed line does not exactly represent expected saturation with respect to fluorite for all samples. It does give the approximate upper boundary of the data, and suggests that fluorite solubility does control fluoride concentrations in the deep geothermal waters.

### Variations in Water Chemistry

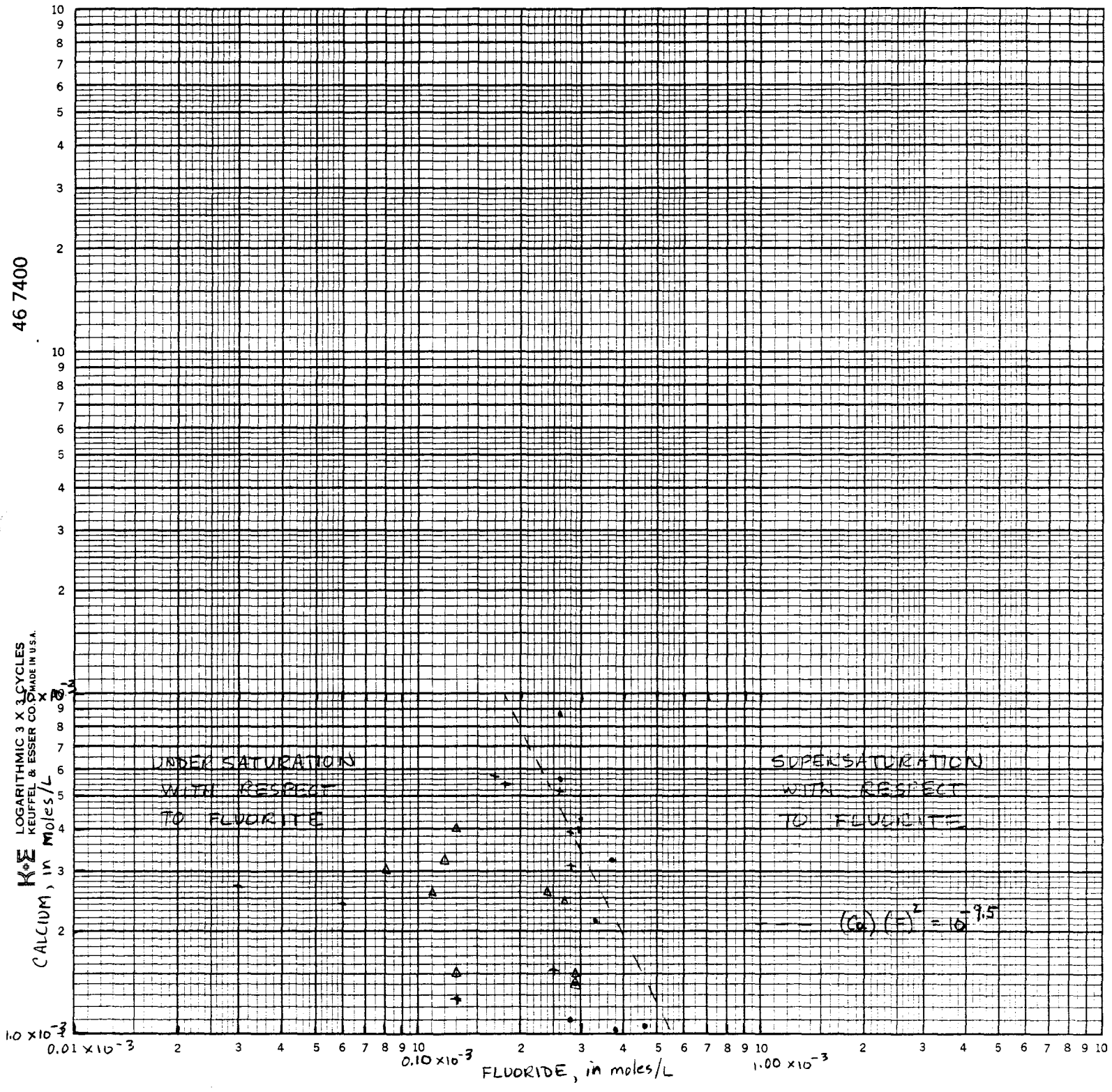
The appearance of the cross sections suggests that cooler, high conductance water moves in from the southeast at a depth between 1200 and 1600 m. This water is warmed as it passes over a heat source between wells RRGE-3 and RRGF-4, and rises by convection to the surface around the crook well. Low dissolved solids water moves in from the northwest, is heated at depth, and rises in the vicinity of the BLM well.

This suggests the presence of two different sources of water to the geothermal reservoir, having very different chemical compositions. An alternative hypothesis, is that the high dissolved solids water is derived from the low dissolved-solids water by concentration due to boiling in the reservoir or extensive alteration of rock material. Figure \_ show oxygen and hydrogen isotopic compositions of ground water, both thermal waters and meteoric waters from nearby springs. Steam separation could produce large shifts in isotopic composition between waters of different dissolved solids concentrations. The graph shows no trends that would support extensive evaporation. There has been insufficient work so far to discount the derivation of salts by alteration of the rock matrix. One line of evidence against this having occurred is the small isotopic shift, which indicates relatively little isotope exchange with rock materials.

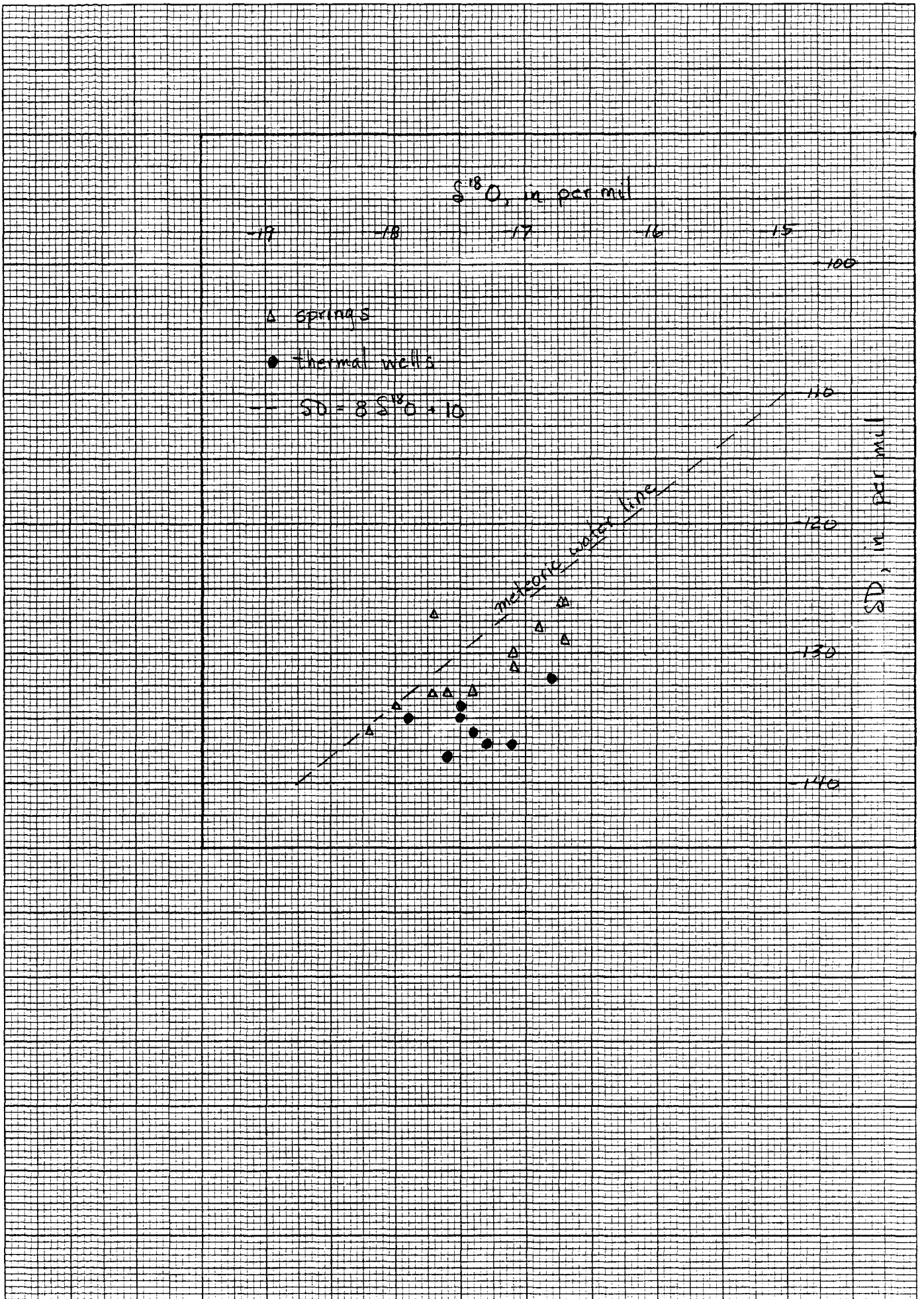
A second line of evidence against the concentration by boiling or leaching is that both require flow of water from a deep ( 1800 meters) zone in the northwest, diagonally upwards to shallower depths to the southeast. Current geologic evidence suggests that structural controls on both movements

46 7400

LOGARITHMIC 3 X 3 CYCLES  
KEUFFEL & ESSER CO. MADE IN U.S.A.



- GEOTHERMAL, BLM, AND CROOK HOT WELLS
- + MONITOR AND USGS WELLS
- Δ IRRIGATION AND DOMESTIC WELLS



probably are oriented in the opposite direction. That is, fracture zones dip towards the southeast.

With two waters having different chemistries, variation in the chemistry of intermediate waters can be due to mixing. This hypothesis was tested by Allen, Chaney, and McAtee (1979) for the Raft River KGRA. The low dissolved solids water from the northwest, they labeled the Bridge-Fault water (type 1), and the high dissolved solids water from the southeast, they labeled the central-valley water (type 2).

Mixing fractions are based on conductivity and calculated using equations

$$X_i C_1 + (1 - X_i) C_2 = C_i \quad (1)$$

or

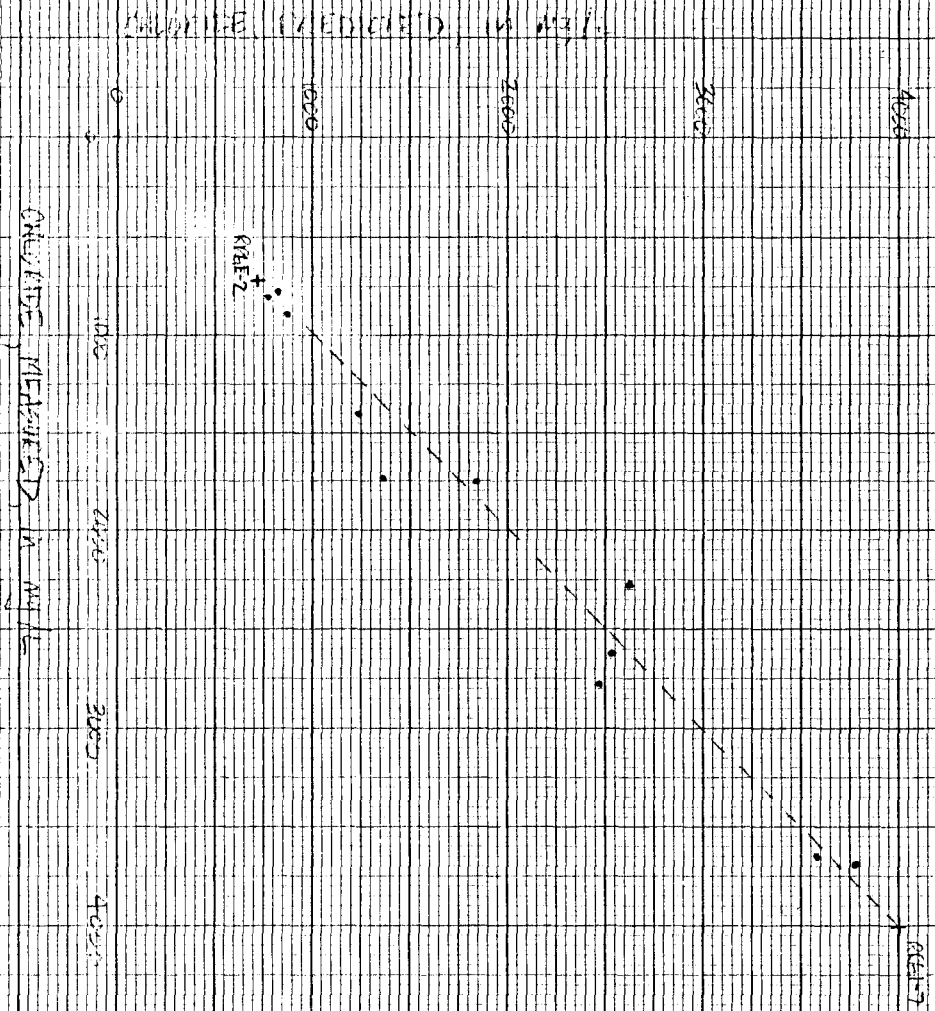
$$X_1 = \frac{C_2 - C_i}{C_2 - C_1} \quad (2)$$

where  $X_i$  is the mixing fraction,  $C_i$  is the conductivity of mixed water,  $C_1$  is the conductivity of Bridge-Fault water (type 1), and  $C_2$  is the conductivity of central-valley water (type 2). For the purpose of this calculation, it is assumed that the lowest conductivity water (from RRGE-2) represents nearly pure Bridge-Fault water ( $C_1$ ) and the highest conductivity water from RRG1-7 represents nearly pure central-valley water ( $C_2$ ). It is recognized that these two waters probably do not represent the actual end-member waters that are mixing. This assumption will not invalidate the calculations for the purpose of mixing for intermediate waters.

Table \_\_\_ shows the mixing fractions calculated by equation (2). Mixing fractions for both deep and intermediate wells are included. In the intermediate zone, the BLM well is the highest fraction of type 1 water and monitor well MW-1 the smallest fraction of type 1 water.

TABLE MIXING FRACTIONS CALCULATED FROM CONDUCTIVITY

	<u>Well</u>	<u>Conductivity</u>	<u>Mixing Fraction of Type 1 Water</u>
Deep	RRGE-2	2500	1.000
	RRGP-5	2700	0.979
	RRGE-1	2800	0.968
-----			
	RRGP-4	4050	0.837
	RRGE-3	8000	0.421
	RRGI-6	10800	0.126
-----			
	RRGI-7	12000	0.000
Inter- mediate	BLM	3000	0.947
	Crook	5800	0.653
-----			
	MW-2	4400	0.800
	MW-6	7600	0.463
	MW-4	7800	0.442
	MW-1	11400	0.063
-----			





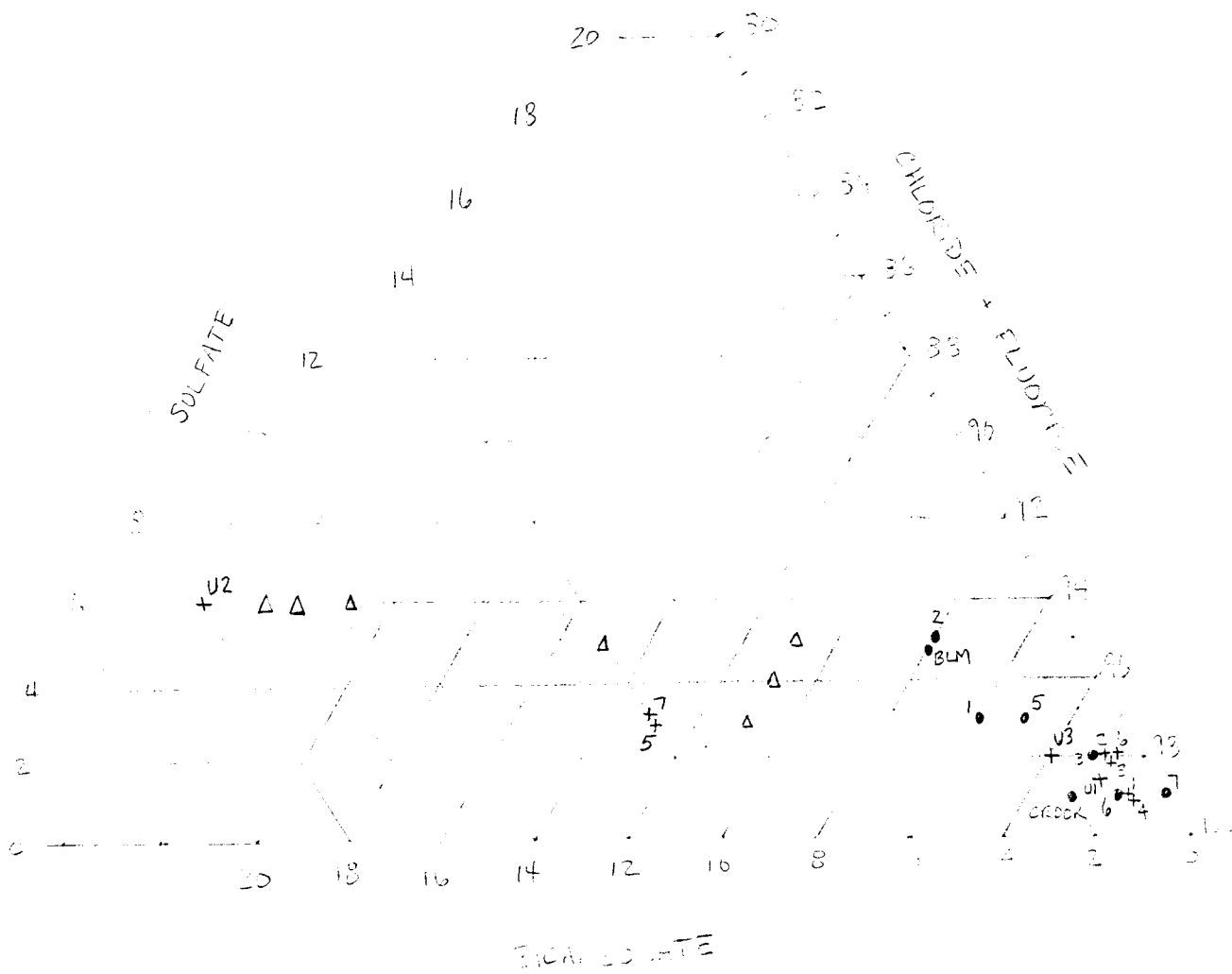
To test the mixing hypothesis, the concentration of chloride in intermediate wells was calculated and compared to measured values. The results, illustrated in Figure \_\_, show generally good agreement between calculated and predicted values.

Trilinear diagrams provide another convenient method for depicting the relations between water samples. Trilinear diagrams show the percent cationic and anionic compositions of water samples in terms of milliequivalents/3 per/liter (meq./L (Hem. 1970)). Figures \_\_ and \_\_ show the trilinear diagrams for cations and anions for ground waters in the vicinity of the Raft River KGRA. Because of ion-exchange reactions that primarily affect cations, the anion trilinear diagram shows relations among water samples much more clearly. Irrigation wells and some of the monitor wells plot along a line crossing the diagram between three and six percent sulfate (Figure \_\_). The slope of this trend changes at the point marked by wells RRGE-2 and BLM. There is a second fairly linear trend between wells RRGE-2 and RRG1-6 and RRG1-7 that depicts mixing in the geothermal reservoir.

The linear trend of the wells across the diagram and the clustering of shallow-monitor and deep-geothermal wells in the same area emphasizes the intrusion of the geothermal waters into the shallow waters. Mixing of geothermal waters with shallow ground waters is an important control on water chemistry.

### Conceptual Model

Figure \_\_ shows a block diagram depicting the movement of water in the Raft River KGRA based on geochemical and geologic evidence. The source of heat for the KGRA is in or below the quartz monzonite in sections 23, 24, 25 and 26 of township 15S, range 26E. There seems to be relatively little water associated with the heat source. Convection above this heat source draws water into the KGRA. Water from the southeast is high in dissolved solids, water from the northwest is low in dissolved solids. Movement is upwards along fracture zones dipping to the southeast associated with the Bridge Fault and various structures. The origin of the low dissolved solids water appears to be from meteoric water based on isotopic composition data. The origin of the high dissolved solids water is still unknown.



- GEOTHERMAL, BLM, AND CROOK WELLS (1-7, BLM, CROOK)
- + MONITOR AND URS WELLS (U1, U2, U3)
- △ HUNTING AND DOMESTIC WELLS



## Conclusions

Geothermal fluids in the Raft River KGRA are derived from two sources of water. Meteoric water from the northwest descends along the valley margin, is heated at depths on the order of 2,000 meters, below (and surface) moves upwards along the Bridge Fault to the surface. Water from the central-valley area, which is high in dissolved solids, is drawn into the KGRA by convection above the heat source. This water reaches the surface in the northwest corner of Section 25, township 15N, range 26E. The chemical variation in the geothermal wells can be explained by mixing of these two waters.

Shallow ground waters also show chemical evidence of mixing of meteoric waters with the higher dissolved solids geothermal waters.

Based on the conceptual model of the Raft River KGRA, the location of the two existing injection wells, RRG1-6 and RRG1-7, is very good for protecting the geothermal resource. However, their location may not be as good in terms of limiting the environmental impact of injection. The injection zone is in the plume of high dissolved solids water moving northwest from the valley center. Increased pressures from injection will increase the rate at which waters in the plume enter the shallow ground water. With more geothermal fluids rising in this area, dilution by shallow waters will decrease, and the dissolved solids in the shallow waters will increase. The limited area currently affected by the rising plume suggests that flow from the southeast is relatively small. The changes in dissolved solids in the shallow ground water expected under an increasing pressure cannot be calculated from current data.